Received: 21 January 2020 | Revised: 5 May 2020 | Accepted: 6 May 2020

DOI: 10.1002/pip.3280

RESEARCH ARTICLE

PROGRESS IN PHOTOVOLTAICS WILEY

Photovoltaic lifetime forecast model based on degradation patterns

Ismail Kaaya[1,3] | Sascha Lindig[2,5] | Karl-Anders Weiss[1] | Alessandro Virtuani[4] | Mariano Sidrach de Cardona Ortin[3] | David Moser[2]

[1]Group Service Life Analysis and Material Characterization, Fraunhofer Institute for Solar Energy, Freiburg, Germany

[2]Institute for Renewable Energy, EURAC Research, Bolzano, Italy

[3]School of Industrial Engineering, University of Malaga, Malaga, Spain

[4]Photovoltaics and Thin Film Electronics Laboratory (PVLAB), Institute of Microengineering (IMT), Swiss Federal Institute of Technology Lausanne, Neuchâtel, Switzerland

[5]Faculty of Engineering, University of Ljubljana, Ljubljana, Slovenia

Correspondence
Ismail Kaaya, Group Service Life Analysis and Material Characterization, Fraunhofer Institute ISE, Heidenhofstr. 2, 79110 Freiburg, Germany.
Email: ismail.kaaya@ise.fraunhofer.de

Funding information
European Commission, Grant/Award Number: 721452

Abstract

The ever-growing secondary market of photovoltaic (PV) systems (i.e., the transaction of solar plants ownership) calls for reliable and high-quality long-term PV degradation forecasts to mitigate the financial risks. However, when long-term PV performance degradation forecasts are required after a short time with limited degradation history, the existing physical and data-driven methods often provide unrealistic degradation scenarios. Therefore, we present a new data-driven method to forecast PV lifetime after a small performance degradation of only 3%. To achieve an accurate and reliable forecast, the developed method addresses the fundamental challenges that usually affect long-term degradation evaluation such as data treatment, choosing a good degradation model, and understanding the different degradation patterns. In the paper, we propose and describe an algorithm for degradation trend evaluation, a new concept of multiple "time- and degradation pattern-dependent" degradation factors. The proposed method has been calibrated and validated using different PV modules and systems data of 5 to 35 years of field exposure. The model has been benchmarked against existing statistical models evaluating 11 experimental PV systems with different technologies. The key advantage of our model over statistical ones is the ability to perform more reliable forecasts with limited degradation history. With an average relative uncertainty of 7.0%, our model is outstanding in consistency for different forecasting time horizons. Moreover, the model is applicable to all PV technologies. The proposed method will aid in making reliable financial decisions and also in adequately planning operation and maintenance activities.

KEYWORDS

degradation, degradation patterns, forecast, lifetime, PV modules, PV systems

1 | INTRODUCTION

Knowing the time period photovoltaic (PV) modules and systems will last, or the remaining useful lifetime (RUL) for operational systems, is of great importance for making good financial decisions as well as planning operation and maintenance activities on PV systems. Despite its importance, it is still a challenge to accurately determine how long a PV module or system will last in real-life operation. Indeed, the lifetime of a PV module or system is influenced by multiple factors such as the local climate, technology, bill of materials and varying

manufacturing, as well as installation quality.[1] In order to accurately determine the lifetime of a PV module or system, it would require monitoring the evolution of power in real-life operation. However, this might require waiting for a significant amount of time. To answer these constraints and needs, mathematical models are utilized to determine the lifetime of PV modules and systems in shorter periods.

On one hand, physical models are used to predict the lifetime of PV modules based on degradation rates evaluated using local climatic stresses[2,3] or based on degradation rates reported from literature.[4] Physical models, especially those based on local climatic stresses, are very helpful to understand the correlation of the predicted performance degradation to different climatic variables. They also aid in analyzing the dominating degradation mechanisms based on local climatic conditions and can be used to map global degradation risk areas, as recently reported in our study.[5] The main challenges of such models are their associated uncertainties and generalizations. The uncertainties could originate from input climatic data, calibration data, model assumptions, and simplifications, which highly effect the prediction accuracy. Currently, there is no standardized way to calculate degradation rates for PV systems. That is why reported values of degradation rates show variations depending on the chosen model and executing research group.[6] The inconsistency between methods and analysts increases the uncertainties in degradation rates evaluation and hence lifetime prediction based on reported values. Moreover, the aforementioned models cannot be easily generalized. They are usually limited to specific module technologies and bills of materials (BOMs). The model parameters need to be re-extracted whenever the modules' BOMs change. The uncertainties associated with technology and geography-specific degradation rates make it difficult to calculate the levelized cost of energy and thus the economic viability of solar energy (Sun et al.[7]).

On the other hand, data-driven techniques that utilize monitored operational data related to system's performance are used in many fields, for example, in the aircraft industry[8,9] to forecast the future trend or the RUL. They are normally applied to complex systems, where developing a physical model could be more complex and expensive. Data-driven techniques can be divided into two categories: statistical techniques (regression methods, autoregressive moving average (ARMA) models, etc.) and artificial intelligence (AI) techniques (neural networks (NNs), fuzzy systems (FSs), etc.).[10]

For PV applications, a few authors have proposed data-driven prognosis models to evaluate the RUL of PV modules. For example, Laayouj et al.[11] proposed a smart prognostic method for PV module health degradation and RUL prediction. The model is based on two approaches: the online diagnosis and the data-driven prognosis. Also, Sheng et al.[12] proposed an ARMA model-filtered hidden Markov model to predict the residual life for complex systems with multiphase degradation. They applied the model to predict the residual life of a specific PV module system. Although both methods are reported to provide good predictions, the main drawback of these methods is that their performances are not rigorously validated or analyzed with different degradation datasets. Both methods are calibrated, validated, and applied based on a single PV module or system dataset. Moreover, for the latter, the methodology was applied to simulated performance measurements for its reliability evaluation and residual life prediction. PV modules can exhibit different degradation scenarios,[13] especially due to different technologies, different failure modes, as well as different operating local climates. Therefore, it is very unlikely that a model calibrated and validated on a single dataset can be generalized to be applicable to other degradation scenarios. In this regard, we propose a model based on a rigorous analysis of degradation data of several PV modules as well as systems of different technologies and installed in different locations. Hence, the proposed model is aimed to be generalized to the different degradation scenarios. Rizzo et al.[14] proposed another algorithm for lifetime extrapolation, prediction, and estimation. However, their algorithm is intended only for emerging PV technologies and for shorter time forecasts.

Generally, in spite of the recognized potential of empirical data-driven techniques for time series forecast, limitations still exist for their application in long-term PV degradation evaluation. Different factors such as outliers in the dataset, seasonal variations, and many other reducing factors (e.g., soiling) should be separated from long-term non-reversible degradation. The lack of a systematic and flexible approach to select parameters of these techniques and their black box character limit the understanding and control of their performance. We address this issue by proposing a systematic and flexible approach with adjustable model parameters to evaluate the degradation trend based on the nature of the dataset under evaluation. The proposed method aims to evaluate the irreversible long-term degradation of PV modules and systems. To achieve this, we propose an iterative algorithm for degradation trends evaluation that allows to separate seasonal variations and other reversible performance reducing effects from irreversible degradation.

Another drawback of the available data-driven techniques is their accuracy when long-term predictions are required after a short time interval and with limited data points. For example, Taylor and Letham[15] performed a comparison of the forecasting accuracy of different statistical models at different time horizons. In their study, most models displayed large uncertainties when applied after shorter time intervals. Indeed, the available techniques are based on fitting the available systems degradation data using regression models and then applying a simple extrapolation to forecast the lifetime. However, in practice, the system's degradation history available may be short and incomplete, and a simple extrapolation could lead to large uncertainties, hence degrading the reliability of the forecasts. To address this challenge, the proposed model is aimed at improving the long-term forecasting accuracy using a small degradation history and few data points. To achieve this, we propose a new concept using time-dependent degradation factors for degradation extrapolation instead of using a simple extrapolation for lifetime forecast. To further improve the accuracy and generalize the model, the concept of multiple degradation factor models, dependent on degradation patterns, is proposed.

The structure of the paper is as follows: in Section 2, the failure time (FT) and the RUL are defined, as well as the proposed modeling approach. While developing a model or an algorithm for lifetime

forecast, the treatment of data is of very high importance to avoid an erroneous lifetime forecasts. Therefore, a significant part in this section is dedicated to data treatment, namely, data filtering, data decomposition, and degradation trend evaluation. As mentioned, it is a fundamental step while developing a model to avoid an erroneous lifetime forecast. The experimental data and methods used in the statistical error analysis are explained as well. In Section 3, the results of the time and degradation pattern model are evaluated. Furthermore, model calibration and validation procedures are presented. Finally, the comparisons of the proposed model with statistical ones as well as its limits, uncertainties, and the prospects of the study are discussed. Finally, the study conclusions are discussed in Section 4.

2 | PROPOSED PV DEGRADATION FORECAST MODEL

2.1 | FT and RUL definitions

Chen Xiongzi et al.[10] defined the RUL of a system or a component as the length from the current time (CT) to the end of its useful life. The question is how to define the "useful life." In this study, the useful life is defined as the non-reversible performance loss, such that the module or system power decreases by 20% of the "maximum stable power" measured in the field. The notion of a maximum stable power is introduced to separate long-term degradation from early stage degradation events such as light-induced degradation (LID) for p-type crystalline silicon modules[13] or light- and elevated temperature-induced degradation for multicrystalline silicon and passivated emitter and rear cell (PERC)[16,17] modules. It also helps to separate other reversible effects reducing module performance such as soiling[18] and seasonal variations.[19] Moreover, due to these effects and variation of the outdoor conditions, the power printed on the PV module label substantially deviates from the initial PV module power outdoors. From our point of view, the maximum stable power can be easily compared among systems and is describing the system performance well, which is not necessarily the case for the nominal power. The nominal power of a PV module/system may deviate substantially from the real power because it is recorded under standard test conditions (STCs). These well-defined conditions of 1000 W/m^2 and 25° C are almost never prevalent as shown in the histogram in Figure 1B.

In this study, we therefore define the FT as a reduction in the module or system performance by 20% of the maximum stable power (indicated by the green dotted line in Figure 1). The 20% loss is purely arbitrary, and it is used in this case because of its consistence with the warranties given by manufacturers. It might be interesting to predict the module or system performance for its entire lifetime (until the module stops working); however, such a prediction could be more unreliable and unrealistic because certain future events are unpredictable. Moreover, the longer a module stays in the field, the more sensitive it becomes to different degradation modes. That might lead to a dramatic increase in the degradation rate, which cannot be easily modeled. According to FT definition, the RUL is the length between the CT to the FT and can be expressed as

$$RUL = FT - CT. \tag{1}$$

2.2 | Power degradation model

Usually, a linear-shaped power loss model with a constant degradation rate throughout the module lifetime is assumed for degradation analysis and lifetime predictions. However, as reported by Jordan et al.[20] non-linearity of power loss is usually observed in the field depending on the module technology and degradation pattern. In their study, the effect of different degradation curves, observed (approximately) in field performance, on the levelized cost of energy (LCOE) was quantified using Monte Carlo simulation. Köntges et al.[13] also reported that the loss in power can take different shapes, for example, exponential-shaped, linear-shaped, step degradation, and saturating power loss over time. In our previous study,[3] a simplified non-linear power degradation function was proposed. This degradation function is selected because of its ability to fit various degradation shapes (DSs) by varying the shape parameter μ as shown in Figure 2A (shapes 1–7

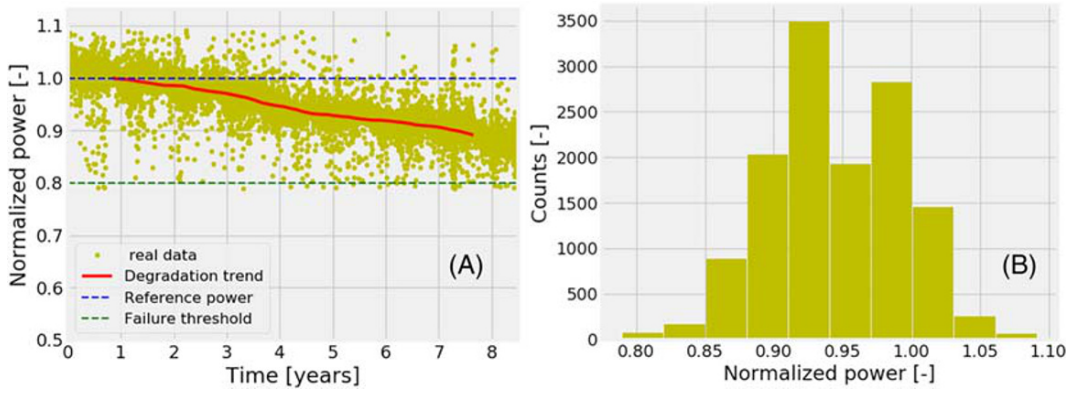

FIGURE 1 A, Illustration of the stable power (red line) used in this study. The green doted line is "maximum stable power" (reference power) and the green dotted is the failure time threshold. B, Histogram of the data distribution throughout the 8.5 years. Power has been normalized to the maximum value of the degradation trend [Colour figure can be viewed at wileyonlinelibrary.com]

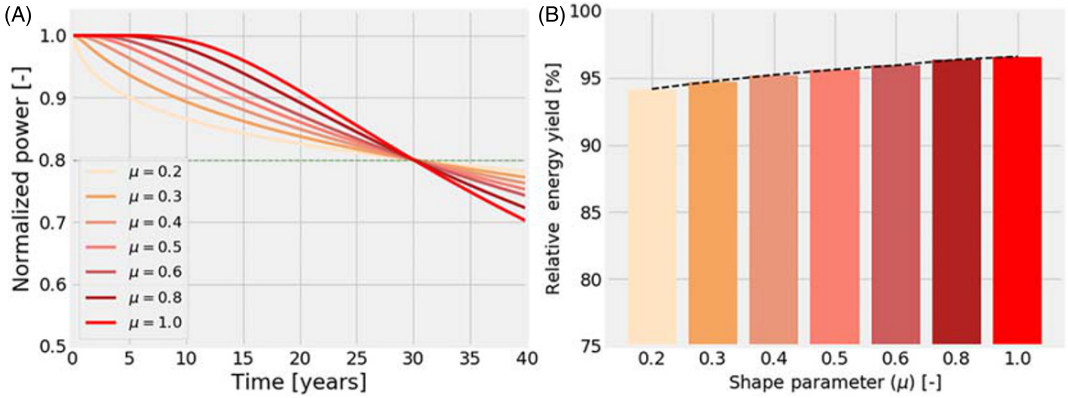

FIGURE 2 A, Optimization of power degradation shapes by altering the shape parameter μ. B, Relative energy yield corresponding to different values of μ [Colour figure can be viewed at wileyonlinelibrary.com]

corresponding to different values of μ= 0.2, 0.3, 0.4, 0.5, 0.6, 0.8, and 1.0, respectively). Moreover, the energy yield could highly depend on the DS even for the same FT as shown in Figure 2B. In this study, the function has been adopted with some modification. It is therefore rewritten as

$$\frac{P(t=t)}{P_{Norm}} = 1 - exp\left(-\left(\frac{1}{k_{cal}t}\right)^{\mu}\right), \tag{2}$$

where P_{Norm} is the maximum power of the degradation trend and k_{cal} is the degradation factor [a^{-1}] at calibration. In this case, the degradation factor is preferred for use instead of the degradation rate because of non-linearity and a non-constant degradation.

TABLE 1 Definition of coefficients and parameters

Coefficients and parameters	Definitions
t_{cal}	Time at calibration threshold
P_{cal}	Power at t_{cal}
$SD_{P_{cal}}$	Standard deviation of calibrated data
$\tau_1 = \sqrt{max(t_{cal})}$	-
$\tau_2 = \lvert ln\Delta t\rvert = \lvert ln(t_{cal} - t_{cal-1})\rvert$	-
$\rho = ln\left(\frac{1}{SD_{P_{cal}}}\right)$	-
A_1 [$year^{-3/2}$], A_2 [$year^{-1/2}$] and A_3 [$year^{-1/2}$]	Proportionality constants
y_1, z_1 and x_1	Optimization parameters

2.2.1 | "Time- and degradation pattern-dependent" models

When evaluating performance degradation of systems with multi-dimensional degradation modes such as a PV system, it is unlikely that a single model holds throughout. On one hand, we assume that different degradation modes and other influencing factors, such as PV module manufacturing defects or defects due to transportation and installation, might cause differences in degradation patterns even for the same BOM and operating conditions. This means that it is unlikely that a single model can represent all expected failure patterns. On the other hand, we assume that some degradation modes might be triggered by other degradation modes and might appear at certain stages of a module's lifetime. This means that using a constant degradation rate extracted at a given stage of PV operation to represent the entire lifetime could affect the forecast accuracy. Taking the aforementioned assumptions into consideration, we propose different degradation factor models dependent on time and degradation pattern. The degradation factor models are expressed as

$$k_1 = k_{cal}\left(1 + A_1.k_{cal}.ln\left(\frac{1}{\Delta P}\right).\tau_1^{y_1}.\tau_2^{x_1}.\rho^{z_1}.t\right) \tag{3}$$

$$k_2 = k_{cal}\left(1 + A_2.k_{cal}.\left(\frac{1}{\tau_1}\right).\rho^{z_1}.t\right) \tag{4}$$

$$k_3 = k_{cal}\left(1 + A_3.k_{cal}.ln\left(\frac{1}{\Delta P}\right).\left(\frac{1}{\tau_1}\right).\tau_2^{x_1}.\rho^{z_1}.t\right). \tag{5}$$

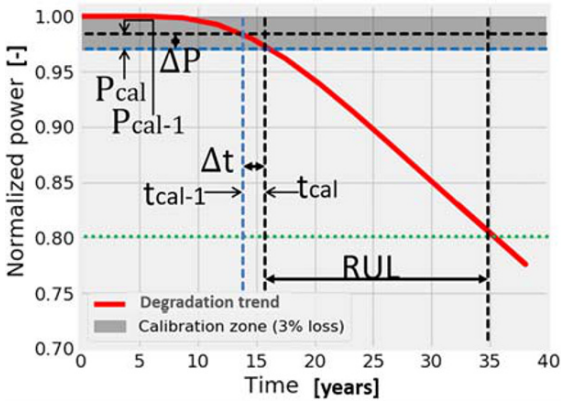

FIGURE 3 Illustration of the different degradation pattern parameters extracted during calibration and the remaining useful lifetime (RUL) [Colour figure can be viewed at wileyonlinelibrary.com]

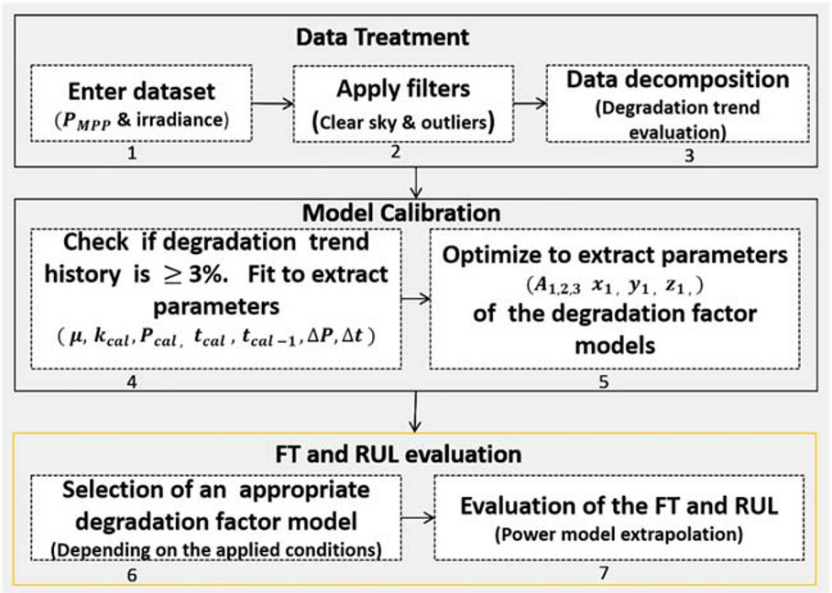

FIGURE 4 Schematic diagram of the modeling approach with three main layers: data treatment, model calibration, as well as FT and RUL evaluation. Note that the 3% degradation history is evaluated from the maximum value of the degradation trend. FT, failure time; RUL, remaining useful lifetime [Colour figure can be viewed at wileyonlinelibrary.com]

The model coefficients and parameters are defined in Table 1. It should be noted that these models are purely empirical without any physical implication; they are derived from degradation pattern parameters shown in Figure 3, as they describe well the specific degradation patterns. It is also important to note that the model parameters are extracted after an initial 3% performance degradation threshold. The 3% optimization threshold is calculated from the degradation trend that excludes early degradation effects. The reasoning for using a 3% threshold is further described and demonstrated in Section 3.

2.3 | Modeling approach

The proposed model has three main steps: data treatment, model calibration, as well as FT and RUL evaluation. These are further divided into seven substeps (see Figure 4).

2.3.1 | Data filtering

The first filter applied to the input dataset is an irradiance filter. The upper limit for irradiance was set and fixed at 1200 W/m^2, and the lower limit was chosen flexible between 600–900 W/m^2, depending on the location under evaluation. This clear sky filter is used as a way to separate low performances due to low irradiance from degradation and also due to its consistence in degradation analysis based on our previous work,[21] where different filters are compared. The filtered power is then corrected to STC of irradiance by applying a linear correction of power to 1000 W/m^2 irradiance. The second step is performed to remove outliers. Because of the stochastic behavior of outdoor conditions and anomalies in the measuring equipment, data measured from outdoor PV modules and systems are usually subject to outliers. When not treated well, outliers might lead to large uncertainties, especially in degradation trend evaluation. The outliers are removed by computing the standard deviation (SD) around the mean value of the entire dataset, whereby all points that are out of the range of (mean ±2× SD) are eliminated. For LID or LeTID sensitive systems, it is a crucial step to analyze the degradation pattern during the first year of operation. These degradation modes are characterized by strong non-linear trends in the initial phase, which might either stabilize gradually or undergo a regeneration phase.[16,17] If a regeneration phase is detected, we recommend to eliminate the data until the onset of this phase.

2.3.2 | Data decomposition

Time series data are characterized by four major components: level, trend, seasonality, and noise. There are two models that are used to model the effects of these components: additive (linear) and multiplicative (non-linear).[22] In our case, a multiplicative model is used. The model suggests that the components are multiplied together as follows:

$$y(t) = Level \times Trend \times Seasonality \times Noise \quad (6)$$

This function is implemented and available for free use in Python.* The function uses a moving average (MA) method to extract a degradation trend in the time series data. The averaging depends on the required resolution (weekly, monthly, or yearly) of one's interest, and it determines the extracted degradation trend in this case.

In outdoor conditions, seasonal and other different effects can reduce the performance of a PV module or system. For non-reversible performance degradation evaluation, it is crucial to choose a good

*librarylinkhttp://www.statsmodels.org/dev/modules/statsmodels/tsa/seasonal.html\#seasonal_decompose

averaging temporal interval that eliminates seasonality and other reversible effects. It has been reported that reversible effects, such as inverter failures and soiling of PV modules, have a higher impact on performance loss rates than the actual performance degradation, which is non-reversible.[23] These effects could be module technology dependent, for example, Virtuani et al.[24] reported that amorphous silicon (a-Si) systems are more affected by variations in the incident spectrum than crystalline silicon (c-Si) systems because of their narrower spectral sensitivity. Therefore, it is important to separate these performance reducing effects from long-term degradation by choosing a good averaging temporal interval. The selection of a good temporal interval could be very tedious if one has to do it manually. An iterative algorithm has been implemented to assist in determining a proper interval for degradation trend evaluation depending on the dataset being evaluated.

2.3.3 | Iterative algorithm for degradation trend evaluation

One way to completely remove any variation in the degradation trend will be to apply a strict constraint, which removes the difference between each nth and (n+1)th value of the trend that is greater or equal to zero, that is, $trend[n-(n+1)] \geq 0$. However, according to the stochastic behavior of outdoor conditions, outdoor measurements usually contain unavoidable outliers that can appear even after applying certain filters. This implies that applying such a strict condition to outdoor dataset is quite unrealistic; in most cases, this condition is not fulfilled or might require a considerable amount of computation time to converge depending on the nature of the dataset. Therefore, a tolerance (tol) is introduced and the condition is applied as

$$trend\left[\left|\frac{max(dn)-min(dn)}{min(dn)}\right|\right] \leq toll,\ for:\ dn = n-(n+1). \quad (7)$$

The process begins by initializing the temporal interval as 2% of the total length of the time series (the 2% is used in this study, but it is adjustable depending on the distribution of the data under evaluation). Afterwards, the iterative loop is repeated until the condition in Equation (7) is fulfilled. The tol depends on the nature of the dataset under investigation, for example, it can be correlated with the resolution of the data or the magnitude of outliers in the datasets. This makes the process of temporal interval selection a quasi-automated process. By analyzing a number of datasets, a range of tol values can be set, granting the flexibility for application on broad datasets of different distributions.

2.4 | Experimental part

Different datasets for PV modules and systems that have been exposed for quite a long period of time with considerable degradation were used in this study. The datasets are from three different sources.

2.4.1 | TIcino SOlare modules

The first set of data are those of the TIcino SOlare (TISO)-10-kW PV plant in Lugano (Switzerland).[25,26] The TISO-10 PV system has been connected to the grid since 1982 and is the oldest installation of this kind in Europe (we shall refer to them as "TISO modules" hereafter). The performance (i.e., current–voltage curves) of 18 selected reference modules was measured at regular intervals between 1982 and 2017. After 35 years in the field, these modules show a degradation rate ranging from −0.2% to −0.7% per year considering a ±3% measurement uncertainty. In this study, 10 of the 18 modules with a considerable degradation have been used in module calibration and validation stages.

2.4.2 | Bolzano systems

Another source of data is a PV plant installed at the airport of Bolzano/Italy (position ∼46.46N, 11.33E, elevation: 262 m), which includes 11 experimental PV systems, which are in operation for 8.5 years during the time period from 01 February 2011 until 31 July 2019. They are referred to as "Bolzano systems." Most major PV system technologies are included, namely, one- and three-junction amorphous silicon (a-Si), cadmium telluride (CdTe), copper indium gallium selenide (CIGS), silicon solar cells made out of a heterojunction with an intrinsic thin layer (HIT), monocrystalline silicon (mc-Si), polycrystalline silicon (pc-Si), and polycrystalline silicon string ribbon (ribbon). All systems are part of one experimental PV plant; they are ground mounted with an orientation of 8.5° southwest and a fixed tilt of 30°. The installed nominal power for the systems range from 1 to 4 kWp per individual installation. According to a new PV sensitive climate classification, proposed by Ascencio-Vázquez et al.[27] the climate in Bolzano is categorized as a temperature climate with medium irradiation. The irradiance is measured with a Kipp & Zonen CMP11 pyranometer. Calibrations are performed in regular intervals, and the measurement uncertainty is between 2% and 4%. Additionally, climate data were taken from a ground-based meteo-station installed in close proximity to the test side.

2.4.3 | Desert Knowledge Australia systems

Finally, data from the Desert Knowledge Australia Solar Centre (DKA Solar Centre),[28] named hereafter as "DKA systems," are used. [†]The datasets used in this study are given as monthly yield in kWh of three different systems; Kyocera-5.4kW-Poly-Si Dual (2008), eco-Kinetics-26.5kW-mono-Si-Dual (2010), and Trina-23.4kw-mono-dual (2009). For the first system (Kyocera), data from 01 January 2009 to 01 December 2018 were used in the analysis; for the eco-Kinetics system, data from 01 January 2011 to 01 December 2018;

[†]The data can be downloaded through https://dkasolarcentre.com.au/locations/alice-springs/graphs?sources=91

and for the Trina system, data from 01 January 2014 to 01 June 2019 were used. More information about these systems and datasets are available on the DKA Solar Centre website. It should be noted that the data plotted here have been normalized to the maximum power and were subject to the outlier filters described in the previous section.

2.5 | Statistical errors analysis

The error measurement employed for the performance evaluation of the proposed forecasting method is the root mean square error (RMSE). Given a measured (m) and a predicted (p) value for a given quantity and number of observations (n), the RMSE is expressed as

$$\sqrt{\frac{\sum_{j=1}^{n}(p_i - m_i)^2}{n}}. \tag{8}$$

The metric deployed to compare the performance of the proposed method with other methods is the relative difference. This is a relative comparison of the FT forecasted after a 3% interval and on the full dataset. It is expressed as

$$Rel_{diff} = \frac{|FT_{3\%} - FT_{full}|}{max(|FT_{3\%}|or|FT_{full}|)}, \tag{9}$$

where Rel_{diff} is the relative difference and $FT_{3\%}$ and FT_{full} are the FT evaluated after a 3% degradation and using the entire dataset, respectively.

3 | RESULTS

3.1 | Time- and degradation pattern-dependent degradation factors and 3% threshold

The power degradation function (Equation 2) was calibrated at different performance degradation intervals (at P = −1%, P = −2%, and P = -3%). At each interval, extrapolation with a constant degradation factor (k_{cal}) was performed and FT was evaluated on two of the TISO modules, namely, TEA5 and TEA6, as shown in Figure 5.

It is clearly visible that although the model fits the data very well at all calibration intervals, the evaluated FT is very different at each calibration interval. This effect is observed for both TEA5 and TEA6 modules. This result demonstrates three aspects: one, a perfectly fitting model does not guarantee better forecast or prediction; two, a model that assumes a constant degradation factor/rate is not appropriate for long-term PV performance degradation forecast; and three, the model forecast accuracy might highly depend on a specific degradation pattern. This effect is visible in the two modules, for example, high discrepancies are visible for the TEA6 module compared with TEA5 module even at similar calibration intervals. Therefore, based on these three observations, the concept of time- and degradation pattern-dependent degradation factor was introduced.

It is also clear that the forecasting accuracy improves as the calibration interval or performance degradation increases, which seems like an obvious observation. However, because the objective is to perform the prediction at the early stages of the module's operation, a 3% threshold was selected. This threshold was found optimal because it provided good forecasts compared with values less than 3% loss. Moreover, another reason is that in situations where the degradation trend is not monotonically decreasing as in many outdoor datasets, using performance degradation of less than 3% might lead to misinterpretation of degradation with seasonal variation or other performance, reducing factors that are reversible. For example, the TEA5 module in Figure 5 shows that prediction after only 1% performance degradation resulted in underestimations compared with the measured degradation trend, which is attributed to the variations in the degradation trend due to reversible effects.

3.2 | Model calibration

The power degradation model (Equation 2) is fitted on measured datasets until 3% loss threshold to extract the model parameters k_{cal} and μ. At the same time, the degradation pattern parameters ΔP, Δt, and t_{cal} are evaluated. To extract the optimization parameters (x_1, y_1,

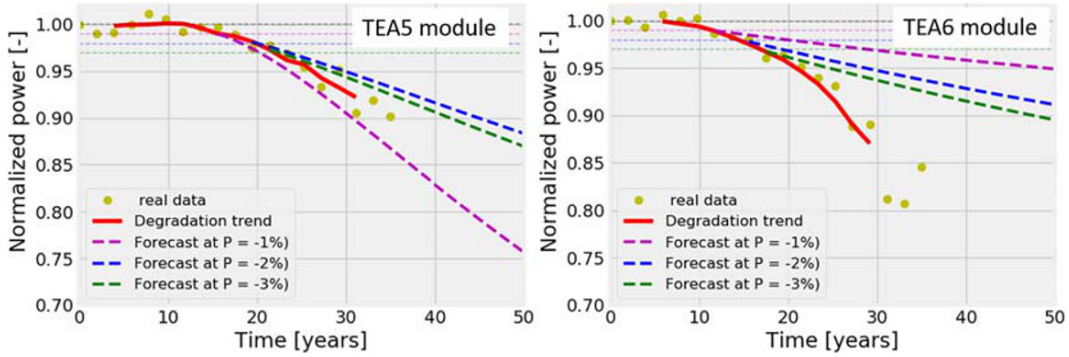

FIGURE 5 Fit and remaining useful lifetime prediction at different percentage power losses of two TIcino SOlare modules, namely, TEA5 and TEA6. The dotted lines represent forecasts at the three calibration intervals [Colour figure can be viewed at wileyonlinelibrary.com]

TABLE 2 Logical conditions for model selection and the corresponding extracted optimization model parameters

Logical conditions	Model	Parameter (y_1)	Parameter (x_1)	Parameter (z_1)
$C_1 : \mu \le 0.35$ & $\Delta P \ge 1.0e{-}4$ & $t_{cal} \le 5$	k_{2c_1}	-	-	3.5
$C_2 : \mu \le 0.45$ & $\Delta P \le 1.0e{-}4$ & $k_{cal} \le 0.009$	k_{3c_2}	-	0.1	1.0
$C_3 : k_{cal} \le 0.013$ & $\Delta P \le 9.5e{-}6$ & $\mu \ge 0.43$	k_{3c_3}	-	0.1	0.5
$C_4 : k_{cal} \ge 0.01$ & $\Delta P \le 5.0e{-}5$ or $\mu \ge 0.75$	$k_{0c_4} = k_{cal}$	-	-	-
$C_5 : \mu \le 0.45$ & $k_{cal} \le 9.0e{-}4$	k_{1c_5}	2.0	1.0	1.0
$C_6 : \mu \le 0.3$ & $\Delta P \ge 0.01$	k_{1c_6}	1.0	0.1	1.0
$C_7 : \mu \ge 0.45$ & $\Delta P \ge 0.01$	k_{1c_7}	1.0	1.5	1.0
$C_8 : \mu \ge 0.45$ & $k_{cal} \ge 0.01$	k_{1c_8}	1.0	0.1	1.0
$C_9 : \mu \ge 0.55$ & $k_{cal} \le 0.005$	k_{1c_9}	-	4.0	1.0
$C_{10} : \mu \le 0.4$ & $\Delta P \le 0.01$ & $k_{cal} \le 0.005$	$k_{1c_{10}}$	-	4.5	1.0
C_{11} : If none of the logical condition are true:	$k_{1c_{11}}$	0.0	2.5	1.0

[a]*Note. C* refers to condition, and the subscripts 1–11 are the number and order of the logical conditions as used in the simulation. k_{jc_i} means calibrate degradation factor model *j* given condition *i*. x_1, y_1, and z_1 are the extracted parameters.

and z_1), the power degradation model is fitted on the extended degradation trend from 3% loss using the degradation factor models (k_1, k_2, and k_3). The proportionality constants (A_1, A_2, and A_3) are all set to one. The extracted power model and degradation pattern parameters are used as the basis to set logical conditions to select which degradation factor model represents a given degradation pattern better. Over 10 logical conditions were created to represent the different degradation patterns as presented in Table 2. These conditions were optimized based on a total of seven TISO modules and two DKA systems. From these modules and systems, different failure patterns were extracted by altering the tol (which changes the degradation trend). Figure 6 shows an example of one of the TISO modules (TEA1) with annual measurements for 35 years and one of the DKA systems (Kyocera system) with monthly average values for 9 years, used for model calibration. It should be noted that despite the strong degradation and huge variations in the data points observed for the DKA systems, they are selected for the calibration process because the objective of the proposed methodology is to be applicable on a wide set of data distribution.

Figure 7A shows the degradation trends of the seven TISO modules used in this study during model calibration. Because an MA smoothening[29] is used to extract the degradation trends, the extracted trends have missing values at the beginning and at the end, because there are no observations on either side. The window of the MA determines the missing values as well as the smoothness of the extracted trend. Generally, the larger the window, the smoother the trend. Figure 7B shows the corresponding change of the degradation factors over time for the seven modules.

It is clearly visible that the rate of degradation factor variation is dependent on the degradation patterns. This is evident for TEA1 module, which displays a strong degradation but with a low rate of change of the degradation factor over time. Furthermore, for some degradation patterns like the one of TEA10, a constant degradation factor (k=k_{cal}) was sufficient to evaluate the long-term degradation. Hence, for such a degradation pattern, it is enough to forecast the lifetime by using only the simplified power degradation model (e.g., Equation 2).

3.3 | Validation

The most important and challenging part of all predictive models is the validation process of the models, which usually requires different sets of measured data than the ones used in the calibration process. In this study, PV modules and systems with a considerable performance degradation were used to validate the performance of the model. At this stage, the raw data are entered in the developed script and the substeps 1 to 7 of Figure 4 are automatically executed. In Figure 8, an elaborative flowchart of steps 6 to 7 is presented. The outcomes are the FT and RUL, as well as a figure. An example is shown in Figure 9 for a Trina and a CIGS system. By comparing the measured trend line and the prediction line, the accuracy of the model was verified.

3.4 | Model application and comparison with ARIMA and Facebook prophet models

The performance of the proposed method is benchmarked against those of two statistical forecasting methods, namely, autoregressive integrated moving average (ARIMA) and Facebook prophet (FP). The reasons for selecting these methods are based on a study by Taylor and Letham,[15] where the performance of the different statistical models in long-term forecast was compared. In their study, FP was found to be outstanding in comparison with other models. The ARIMA model was characterized with the highest uncertainties. We selected the best and the least performing models to compare the accuracy of the proposed model and to investigate whether the nature of the data under evaluation could affect the models' performance. Moreover, both methodologies are simple to apply and commonly used in

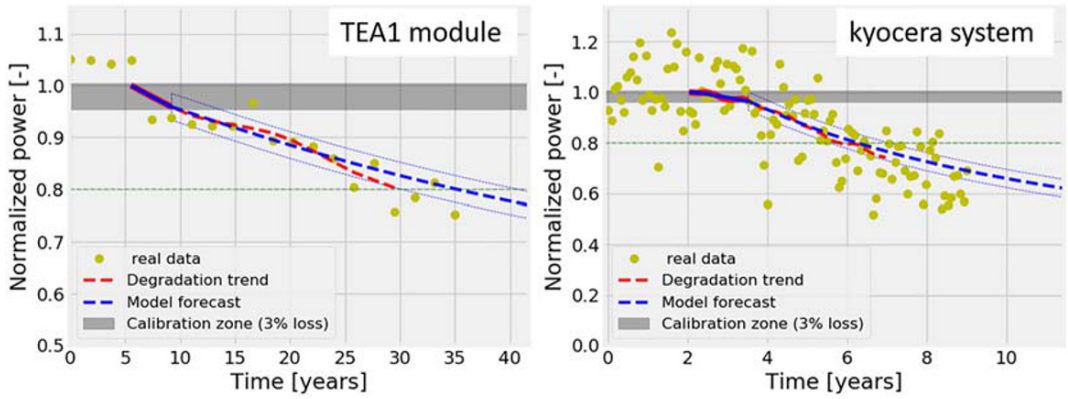

FIGURE 6 TEA1 module (from the TIcino SOlare modules) and Kyocera system (from Desert Knowledge Australia systems) selected for calibration. In yellow are the measurements, red dashed line shows the extracted degradation trend, and the thick blue line is the model prediction with the 95% confidence interval shown using blue dotted lines. The horizontal green dotted line shows the −20% failure threshold of the degradation trend. Power has been normalized to the maximum value of the degradation trend [Colour figure can be viewed at wileyonlinelibrary.com]

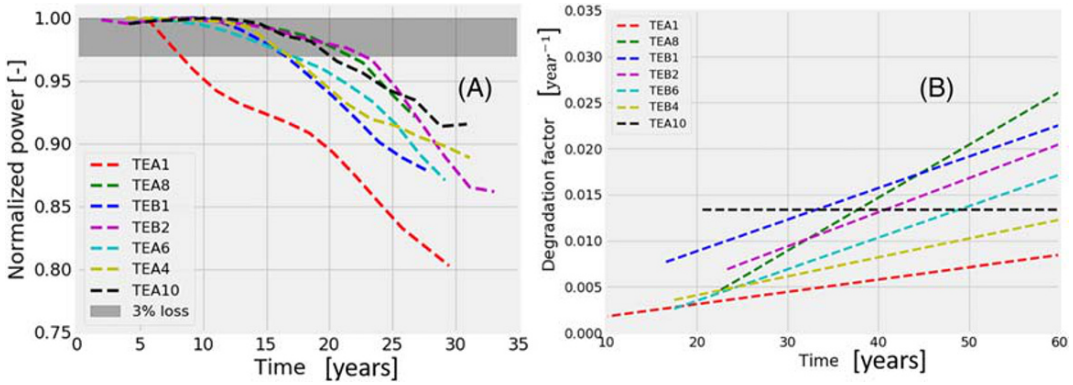

FIGURE 7 A, Different TIcino SOlare modules used in model calibration. B, Change of the degradation factor over time of the seven modules, respectively [Colour figure can be viewed at wileyonlinelibrary.com]

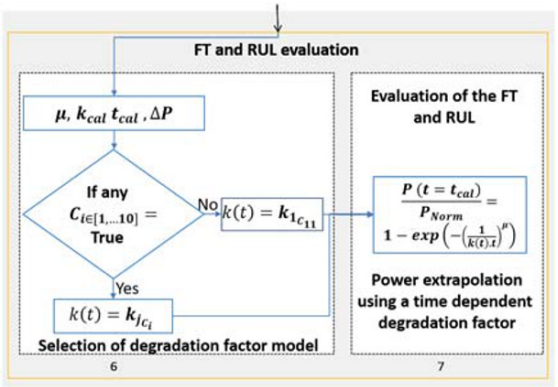

FIGURE 8 Flowchart illustrating the selection of degradation factor model and power extrapolation steps . $k(t) = k_{jc_i}$ is the calibrated time-dependent degradation factor model $j\in[1,...,3]$ given condition $C_{i\in[1,...,10]}$. This figure is an elaborative part of steps 6 and 7 of Figure 4 [Colour figure can be viewed at wileyonlinelibrary.com]

different fields. For example, the FP algorithm is implemented in common programming languages such as Python and R. [‡] The methodology was created as a flexible time series model that is configurable by non-experts. It is based on a decomposable time series model including trend, seasonality, holidays (not important for our application), and an error term. The model gives the opportunity to choose linear and logistic time series evolution, the second being suited for the nonlinear behavior of PV performance. Furthermore, among the seasonality settings for different time resolutions, yearly seasonality was selected to detect yearly variations in power production due to the seasons of a year. The ARIMA model has free online packages.[30,31] In this study, an auto-ARIMA function that uses the Akaike information criterion (AIC) to get the optimal model was used.

[‡]The code can be accessed at https://facebook.github.io/prophet/

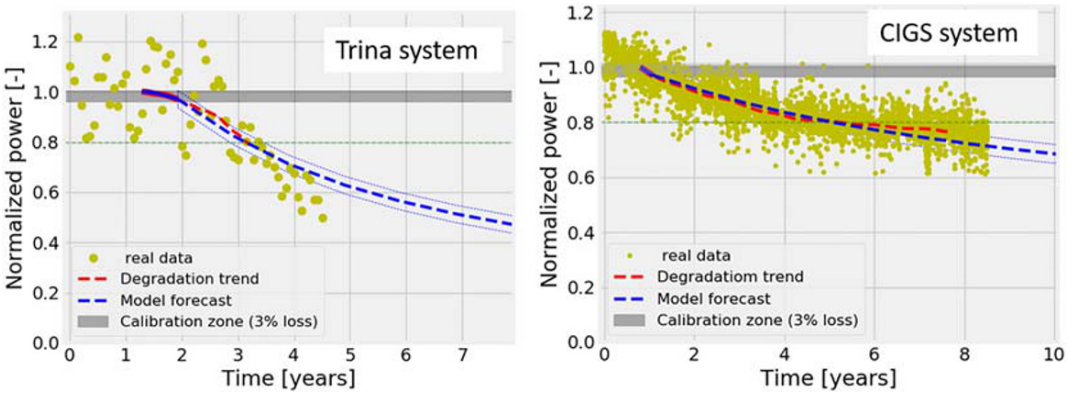

FIGURE 9 Model validation with experimental datasets of Trina system and copper indium gallium selenide (CIGS system). In yellow are the measurements, the red dashed line shows the extracted degradation trend, and the thick dashed blue line is the model prediction with the 95% confidence interval shown in blue as well. The horizontal green dotted line shows the −20% failure threshold of the degradation trend. Power has been normalized to the maximum value of the degradation trend [Colour figure can be viewed at wileyonlinelibrary.com]

The performance evaluation is carried out using the 11 Bolzano system datasets. The comparison of the three models is twofold: first, the models are compared on the lifetime forecast after a small performance degradation interval and second, on the consistency of the forecast at two different forecasting intervals. In the first attempt, the same system input data (normalized and STC irradiance corrected power time series with 3% performance degradation as training data) were tested on ARIMA and FP models. Unfortunately, no meaningful predictions were achieved because the number of calculated change points is greater than the number of observations in the dataset. Instead, the monthly performance ratio (PR) was used as the input parameter. The PR sets the actual yield of a PV system in relation with the expected yield at STC conditions.[32] For model comparison, the models are calibrated at two different intervals: first , at an interval corresponding to the 3% performance degradation and second, using the entire datasets corresponding to the 8.5-year interval. The respective lifetime and RUL forecasts are shown in Table 3.

Considering a 3% calibration threshold, it is clear that there are high discrepancies in the FT forecast among the three models. It is also observed that the FTs are either overestimated or

TABLE 3 Comparision of ARIMA, Facebook prophet, and the proposed model at two prediction intervals

System	HIT1	mc-Si1	mc-Si2	pc1	pc2	pc3	1j	3j	ribbon1	CdTe1	CIGS1
ARIMA											
$FT_{3\%}$ (years)	19.5	NA	16.8	9.1	12.2	16.0	15.3	NA	12.2	14.4	NA
$RUL_{3\%}$ (years)	11.0	NA	8.3	0.6	3.8	7.5	6.8	NA	5.3	5.9	NA
FT_{full} (years)	19.3	NA	13.2	NA	19.1	22.9	14.0	NA	19.1	11.1	2.1
RUL_{full} (years)	10.8	NA	4.8	NA	10.6	14.4	5.5	NA	10.6	2.6	−6.4
Rel_{diff} (%)	1.0	–	21.4	NA	36.1	30.1	8.5	–	36.1	22.9	NA
Facebook prophet											
$FT_{3\%}$ (years)	32.1	34.5	12.8	8.9	8.7	13.9	14.3	18.6	8.7	13.4	NA
$RUL_{3\%}$ (years)	23.6	26.0	4.3	0.4	0.2	5.4	5.8	10.1	0.2	4.9	NA
FT_{full} (years)	15.6	34.5	13.6	27.2	21.1	16.8	14.0	18.6	21.5	11.5	3.0
RUL_{full} (years)	7.1	26.0	5.1	18.8	12.6	8.2	5.5	10.1	13.0	3.0	−5.4
Rel_{diff} (%)	51.4	–	5.8	67.3	58.8	17.3	2.1	–	59.5	14.1	NA
Proposed											
$FT_{3\%}$	15.9	74.3	16.5	15.5	21.6	23.8	16.7	23.7	21.2	14.0	5.0
$RUL_{3\%}$ (years)	7.4	65.7	8.0	7.0	13.1	15.3	8.2	15.2	12.7	5.5	−3.5
FT_{full} (years)	15.2	74.3	16.5	14.1	21.1	17.8	18.8	23.7	20.5	13.9	5.6
RUL_{full} (years)	8.3	65.7	8.0	5.6	12.2	9.3	10.3	15.2	12.0	5.4	−2.9
Rel_{diff} (%)	4.4	–	0	9.2	2.3	24.8	7.2	–	3.3	0.7	10.7

[a]*Note.* $FT_{3\%}$ & FT_{full} are failure times calculated using 3% degradation and the compelete datasets, respectively. 1j is 1j-a-Si1, 3j is 3j-a-Si1, pc1 is pc-Si1, pc2 is pc-Si2, and pc3 is pc-Si3.

[b]Abbreviations: ARIMA, autoregressive integrated moving average; CdTe, cadmium telluride; FT, failure time; HIT, heterojunction with an intrinsic thin layer; mc-Si, mono-crystalline silicon; pc, polycrystalline silicon; ribbon, polycrystalline silicon string ribbon; RUL, remaining useful lifetime.

underestimated for the ARIMA and FP models. The overestimations and underestimations can be correlated with the evaluated degradation trend, which is influenced by the nature of the dataset and the number of data points. Considering the calibration using the entire dataset, the FP and the proposed model show good agreement in the FT forecast for most of the systems. This excludes the mc-Si1 system that appeared to be very stable with a performance degradation of less than 2% after 8.5 years. For this system, the proposed model shows an overestimation of the FT because the evaluated degradation is too small to achieve optimal calibrations. Comparing the variations in predictions at different calibration intervals, it can be seen that the proposed model displays a good consistency (on average, 7% relative difference) compared with the other two models that displayed unrealistic scenarios. Although the FP showed a good agreement with the proposed model when calibrated using the entire dataset, it displayed big variations in lifetime forecast between the two calibration intervals. Considering both intervals, the ARIMA model does not perform well in this study because it failed to converge for four systems. The model also tends to overfit the data, hence making it more sensitive to reversible performance reducing events. This is visible when looking at the pc-Si1 system (Figure 10) where the model failed to converge when calibrated on the entire dataset. This implies that such a model is not useful for performance degradation forecast.

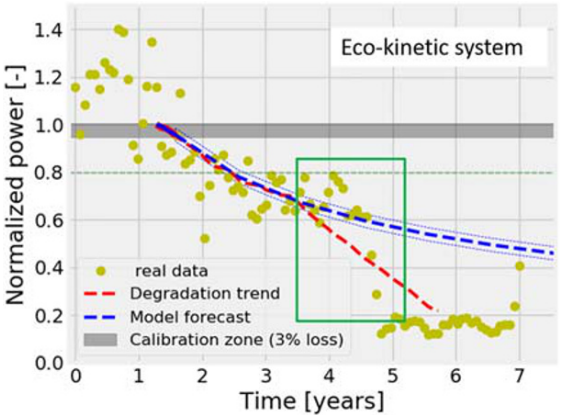

FIGURE 11 System showing a sudden drop in power (around the green box). In blue is the model forecast. The horizontal green dotted line shows the −20% failure threshold of the degradation trend. Power has been normalized to the maximum value of the degradation trend [Colour figure can be viewed at wileyonlinelibrary.com]

3.5 | Model limits and uncertainties

Although the proposed model has displayed a good performance on a number of PV modules and systems, it is bound to some limits and uncertainties that could deteriorate the prediction accuracy. The model limits and uncertainties are identified as follows.

The model works well when the degradation is gradual and continuous. It cannot forecast events that might lead to dramatic or sudden power losses, such as breakage, fire, or catastrophic failures. For example, Figure 11 shows one of the DKASC Alice Spring systems; eco-Kinetics-26.5kW-mono-Si-Dual (2010), which experiences a sudden drop in performance. According to the information from the DKA website, this sharp drop in performance was attributed to one PV module in the array being subject to damage during a windstorm. The cause is identified as a partial failure of one array string in which this damaged module is connected.

The model is based on degradation patterns; hence, it is influenced by the extracted degradation trends. The degradation trend is extracted from time series data by applying the condition in Equation (7). Changing the tol value affects the extracted degradation trend as shown in Figure 12A. Figure 12B shows how the calibration and the forecast error vary with tol. The RMSE was calculated using Equation (8) and is converted to percentage.

According to the evaluated datasets in this study, the value of tol and the extracted degradation trend highly depend on the resolution and the outliers in a given dataset. For datasets with a monthly or yearly resolution, the values of tol ranged from 0.9 to 1.25, whereas for datasets with high resolution of 15 min, the values were between

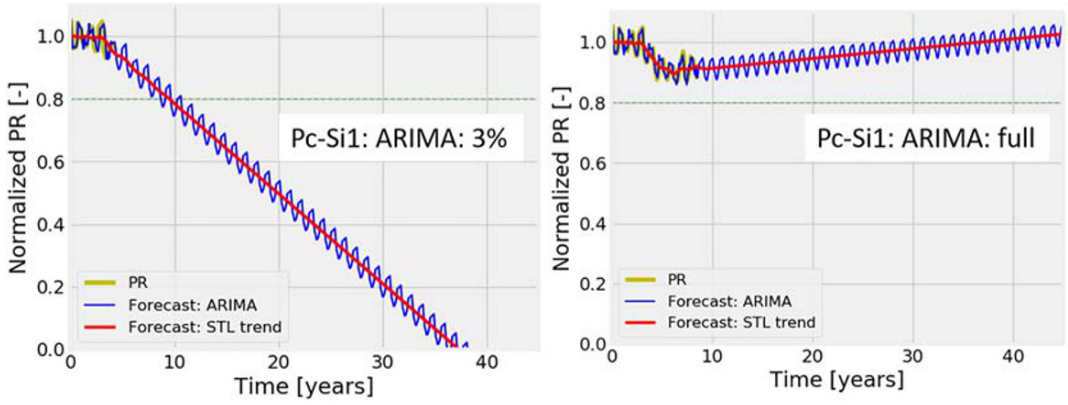

FIGURE 10 Forecast at 3% and entire dataset calibration thresholds using auto-ARIMA model. The figure shows overfitting when calibration is done on the entire dataset. The green dotted line shows the −20% failure threshold of the Seasonal–Trend Decomposition Using LOESS (STL) . PR has been normalized to the initial value of the STL trend. ARIMA, autoregressive integrated moving average; PR, performance ratio [Colour figure can be viewed at wileyonlinelibrary.com]

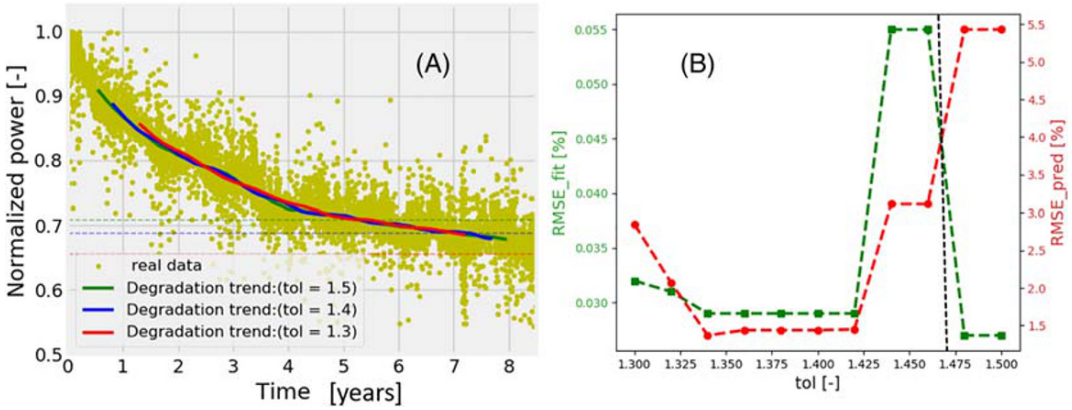

FIGURE 12 A, Variation of the extracted degradation at different values of tol. The horizontal dotted lines show the −20% failure threshold of the degradation trend. Power has been normalized to the maximum value of the real data. B, Variation of the fitting error (RMSE_fit) and forecast error (RMSE_pred) with different values of tol. RMSE, root mean square error; tol, tolerance [Colour figure can be viewed at wileyonlinelibrary.com]

1.4 and 1.65. The tol factor is very useful as it provides a parameter for optimization adapted to the dataset variability unlike the black box automated algorithms.

3.6 | Prospects

After optimizing, testing, and further validating our model under different data scenarios, the overall objective is to embed the approach into a simplified user interface for PV lifetime forecast. The interface will be applicable by any user, even without deep knowledge in data analysis. The next step will be to interpret the derived model parameters dependent on the degradation patterns to the degradation modes. We believe that with enough PV modules and systems data, it is possible to correlate the degradation patterns with degradation modes based on PV technologies, operating local climate, and BOM. Meanwhile, this paper will serve as a guideline for anyone willing to go through and apply the presented modeling approach and algorithms. Moreover, it can trigger ideas to build new or modify available algorithms to achieve the highest accuracy in PV lifetime predictions and forecasting.

4 | CONCLUSION

Degradation rate models based on local climatic stresses and data-driven models based on the existing monitored degradation to forecast the lifetime of PV modules have already been proposed. However, climatic-based models are characterized by too many sources of uncertainties due to many input variables and the available data-driven forecast models are characterized by high uncertainty when long-term forecasts are required after a shorter time and with few data points. If only an insufficient number of data points is available, data-driven models are not able to capture the real trend of the dataset and will be dominated by short-term effects in the dataset, which might not represent the actual performance evolution of a PV system. In this paper, we provide a solution to these key challenges by proposing a simplified model that requires less input variables and aims at improving the accuracy of long-term forecasts after a shorter operation time and with fewer data points. The proposed approach is based on multiple time- and degradation pattern-dependent models to evaluate the long-term performance degradation.

The proposed model has been calibrated and validated using different PV module and system datasets with observed long-term degradation. The performance of the proposed model is benchmarked against two statistical methods, namely, ARIMA and FP, using the time series of 11 experimental PV plants (with different PV technologies). The proposed model displays outstanding performance when forecasts are made after a shorter time compared with the two statistical models that displayed unrealistic forecasts. The model also displays consistent results with a 7.0% average relative uncertainty of the evaluated FT when forecasts are made at different intervals, which is not the case for the two statistical models. Therefore, the obvious advantage of the proposed model over other data-driven models is that it is applicable after a small performance degradation of only 3%, which usually can be observed after a short operation time. Furthermore, it is applicable on fewer data points. Another advantage of the proposed approach is that it is based on a systematic strategy as well as for selecting the data and parameters of the models, making it applicable for degradation evaluation on a wide range of data distributions. The models' performance can be well understood and a correlation of different parameters can be achieved, which is not the case for many empirical, data-driven techniques, especially those with a black box character. Moreover, the model is also applicable to all PV technologies.

The paper also highlights the pitfalls of assuming a single constant degradation factor/rate for long-term PV performance degradation forecast/ prediction. It has been shown that using a constant degradation factor/rate might lead to either overestimation or underestimation of the FT and that this depends on the degradation patterns. We

believe that accurate PV lifetime forecast/prediction is of great importance in the ever-growing secondary market of PV systems (i.e., the transaction of ownership of solar plants), as a metric to evaluate financial figures and mitigate risk.

ACKNOWLEDGEMENTS

This work has received funding from the European Commission, Research Executive Agency (REA) under the Marie Sklodowska-Curie Innovative Networks, grant agreement no. 721452-Project SolarTrain. The authors are sincerely grateful and would like to acknowledge the Scuola Universitaria Professionale della Svizzera Italiana (SUPSI) for sharing the TISO plant data, which were very useful inputs for this analysis. We would also like to acknowledge and appreciate the Desert Knowledge Australia Solar Centre's (DKA Solar Centre) continuous effort to provide free access of photovoltaic systems data.

CONFLICT OF INTEREST

The authors declare no conflict of interest.

ORCID

Ismail Kaaya https://orcid.org/0000-0003-4524-0975
Sascha Lindig https://orcid.org/0000-0001-5421-8265
Alessandro Virtuani https://orcid.org/0000-0001-5523-5200

REFERENCES

1. Jordan DC, Silverman TJ, Wohlgemuth JH, Kurtz SR, VanSant KT. Photovoltaic failure and degradation modes. *Prog Photovolt Res Appl*. 2017;25(4):318-326.
2. Bala Subramaniyan A, Pan R, Kuitche J, TamizhMani G. Quantification of environmental effects on PV module degradation: a physics-based data-driven modeling method. *IEEE J Photovolt*. 2018;8(5):1289-1296.
3. Kaaya I, Köhl M, Mehilli A, Mariano SdC, Weiss KA. Modeling outdoor service lifetime prediction of PV modules: effects of combined climatic stressors on PV module power degradation. *IEEE J Photovolt*. 2019;9:1105-1112.
4. Vázquez M, Rey-Stolle I. Photovoltaic module reliability model based on field degradation studies. *Prog Photovolt Res Appl*. 2008;16(5):419-433.
5. Ascencio-Vásquez J, Kaaya I, Brecl K, Weiss KA. Topic M. Global climate data processing and mapping of degradation mechanisms and degradation rates of PV modules. *Energies*. 2019;12(24):4749.
6. Jordan DC, Deline C, Deceglie MG, et al. Reducing interanalyst variability in photovoltaic degradation rate assessments. *IEEE J Photovolt*. 2020;10(1):206-212.
7. Sun X, Chavali RVK, Alam MA. Real-time monitoring and diagnosis of photovoltaic system degradation only using maximum power point-the Suns-Vmp method. *Prog Photovolt Res Appl*. 2019;27(1):55-66.
8. Zhang S, Zhang Y, Zhu J. Residual life prediction based on dynamic weighted Markov model and particle filtering. *J Intell Manu*. 2018;29(4):753-761.
9. Listou Ellefsen A, Bjørlykhaug E, Æsøy V, Ushakov S, Zhang H. Remaining useful life predictions for turbofan engine degradation using semi-supervised deep architecture. *Reliab Eng Sys Safe*. 2019;183:240-251.
10. Chen X, Yu J, Tang D, Wang Y. Remaining useful life prognostic estimation for aircraft subsystems or components: a review. In: IEEE 2011 10th International Conference on Electronic Measurement Instruments, Vol. 2; 2011:94-98.
11. Jamouli H, Hail ME. Intelligent prognostic framework for degradation assessment and remaining useful life estimation of photovoltaic module. *J Eng Tech Sci*. 2016;48(6):772-795–795.
12. Sheng Z, Hu Q, Liu J, Yu D. Residual life prediction for complex systems with multi-phase degradation by ARMA-filtered hidden Markov model. *Qual Tech Quan Manage*. 2019;16(1):19-35.
13. Köntges M, Kurtz S, Packard CE, et al. Review of Failures of Photovoltaic Modules. IEA International Energy Agency; 2014.
14. Rizzo A, Cester A, Madsen MV, Krebs FC, Gevorgyan SA. A novel algorithm for lifetime extrapolation, prediction, and estimation of emerging PV technologies. *Small Method*. 2018;2(1):1700285.
15. Taylor SJ, Letham B. Forecasting at scale. *American Stat*. 2018;72(1):37-45.
16. Kersten F, Fertig F, Petter K, et al. System performance loss due to LeTID. *Energy Procedia*. 2017;124:540-546. http://www.sciencedirect.com/science/article/pii/S1876610217341917
17. Philipp D, Geipel T, Gebhardt P, Schmid A, Naeem T, Fokuhl E. LeTID—A Comparison of Test Methods on Module Level. In: 36th European Photovoltaic Solar Energy Conference and Exhibition; 2019:816-821. http://www.eupvsec-proceedings.com/proceedings?paper=48290
18. Zorrilla-Casanova J, Piliougine M, Carretero J, et al. Losses produced by soiling in the incoming radiation to photovoltaic modules. *Prog Photovolt Res Appl*. 2013;21(4):790-796.
19. Cañete C, Carretero J, Sidrach-de Cardona M. Energy performance of different photovoltaic module technologies under outdoor conditions. *Energy*. 2014;65:295-302.
20. Jordan DC, Silverman TJ, Sekulic B, Kurtz SR. PV degradation curves: non-linearities and failure modes. *Prog Photovolt Res Appl*. 2017;25(7):583-591.
21. Kaaya I, Betts TR, Lindig S, et al. Service Lifetime Prediction of PV Modules and Systems: Progress of the SOLAR-TRAIN Project. In: 2019 IEEE 46th Photovoltaic Specialists Conference (PVSC) Chicago, IL, USA: IEEE; 2019:1352-1356. https://ieeexplore.ieee.org/document/8980791/.
22. Brownlee J. Introduction to Time Series Forecasting With Python: How to Prepare Data and Develop Models to Predict the Future. Machine Learning Mastery; 2017.
23. Klünter C, Rauschen I, Reinartz K, Müller B, Farnung B, Kiefer K. Degradation in PV Power Plants: Theory and Practice. In: 36th European Photovoltaic Solar Energy Conference and Exhibition; 2019:1331-1335.
24. Virtuani A, Strepparava D, Friesen G. A simple approach to model the performance of photovoltaic solar modules in operation. *Solar Energy*. 2015;120:439-449.
25. Virtuani A, Caccivio M, Annigoni E, et al. 35 years of photovoltaics: analysis of the TISO-10-kW solar plant, lessons learnt in safety and performance—part 1. *Prog Photovolt Res Appl*. 2019;27(4):328-339.
26. Annigoni E, Virtuani A, Caccivio M, Friesen G, Chianese D, Ballif C. 35 years of photovoltaics: analysis of the TISO-10-kW solar plant, lessons learnt in safety and performance—part 2. *Prog Photovolt Res Appl*. 2019;27(9):760-778. https://onlinelibrary.wiley.com/doi/abs/10.1002/pip.3146
27. Ascencio-Vásquez J, Brecl K, Topic M. Methodology of Köppen-Geiger-Photovoltaic climate classification and implications to worldwide mapping of PV system performance. *Solar Energy*. 2019;191:672-685. http://www.sciencedirect.com/science/article/pii/S0038092X19308527
28. Dkasc AS. DKASC, Alice Springs | DKA Solar Centre |. http://dkasolarcentre.com.au/locations/alice-springs, 2019-11-08 http://dkasolarcentre.com.au/locations/alice-springs; 2019.
29. Hyndman JR, Athanasopoulos G. Forecasting: Principles and Practice. 2nd edition ed. https://Otexts.com/fpp

30. Hyndman RJ, Athanasopoulos G, Bergmeir C, et al. forecast: Forecasting Functions for Time Series and Linear Models version 8.10 from CRAN. https://rdrr.io/cran/forecast
31. Hyndman RJ, Khandakar Y. Automatic time series forecasting: the forecast package for R. *J Stat Soft*. 2008;27(1):1-22. https://www.jstatsoft.org/index.php/jss/article/view/v027i03
32. IEC61724-1. Photovoltaic system performance, Part 1: Monitoring. Geneva, CH: International Electrotechnical Commission; 2017; 2017.

How to cite this article: Kaaya I, Lindig S, Weiss K-A, Virtuani A, Sidrach de Cardona Ortin M, Moser D. Photovoltaic lifetime forecast model based on degradation patterns. *Prog Photovolt Res Appl*. 2020;1–14. https://doi.org/10.1002/pip.3280